Algal Research 12 (2015) 91–98

Contents lists available at ScienceDirect

Algal Research

journal homepage: www.elsevier.com/locate/algal

Enhancing plasma membrane NADPH oxidase activity increases current output by diatoms in biophotovoltaic devices

Anuphon Laohavisit [a,1], Alexander Anderson [a,2], Paolo Bombelli [b], Matthew Jacobs [a,3], Christopher J. Howe [b], Julia M. Davies [a], Alison G. Smith [a,*]

[a] Department of Plant Sciences, Downing Site, University of Cambridge, CB2 3EA, UK
[b] Department of Biochemistry, University of Cambridge, CB2 1QW, UK

ARTICLE INFO

Article history:
Received 3 January 2015
Received in revised form 11 August 2015
Accepted 15 August 2015
Available online 31 August 2015

Keywords:
Photosynthetic fuel cell
Diatoms
Superoxide anion
NADPH oxidase

ABSTRACT

Biophotovoltaic (BPV) devices employ the photosynthetic activity of microalgae or cyanobacteria to harvest light energy and generate electrical current directly as a result of the release of electrons from the algal cells. NADPH oxidases (NOX) are plasma-membrane enzymes that transport electrons from the cytosol to generate extracellular superoxide anions, and have been implicated in BPV output. In this study, we investigated NOX activity in the diatoms *Phaeodactylum tricornutum* and *Thalassiosira pseudonana* in an attempt to understand and enhance NOX and BPV function. We found that NOX activity was linked to defined growth regimes and growth phases, and was light dependent. Crucially, current output in a BPV device correlated with NOX activity, and levels of up to 14 μA per 10^6 cells (approximately 500 $mA \cdot m^{-2}$) were obtained. Expression of two putative *P. tricornutum* NOX genes (*PtNOX1* and *PtNOX2*) was found to correspond with the observed growth patterns of superoxide anion production and power output, suggesting that these are responsible for the observed patterns of NOX activity. Crucially, we demonstrate that NOX activity levels could be enhanced via semi-continuous culturing, pointing to the possibility of maintaining long-term power output in BPV devices.

1. Introduction

To cope with an increasing world population and energy demand there has been extensive research into new ways of exploiting renewable biological sources of energy [1]. One such technology is the microbial fuel cell, which makes use of electron-producing catalytic processes in heterotrophic microbes to generate electricity [2]. The electrons are harvested from metabolic by-products of microbial respiration. However, this requires a continuous source of organic carbon to support metabolism. An alternative is to operate such devices with photosynthetic microorganisms such as microalgae and cyanobacteria, which require only sunlight as energy and water as a source of electrons, converting these into electricity and creating, in essence, a biological solar panel [2]. In such devices (termed biological photovoltaic (BPV) devices [3]), electrons are extracted from water by the photosynthetic machinery and are transported to and across the outer cell membranes [4]. Electrons can be harvested either via a soluble electron carrier included in the aqueous medium [3] or directly from the cell surface by growing algae as biofilms onto the anode [5]. In both cases electrical output is sustained over long periods but overall power output levels remain low, with the highest so far reported being in the region of 100 mW m^{-2} for a biofilm of the cyanobacterium *Synechocystis* PCC6803 [6]. Investigating how electrons are sourced, transported and extruded from cells could lead to improvements in BPV power output. The plasma membrane is a significant barrier for electron extrusion, so studying mechanisms for electron transport across this membrane will be key for understanding how algal cells operate in BPV devices.

For heterotrophic microorganisms in microbial fuel cells several mechanisms have been considered, including self-excreted endogenous electron carriers and biological nano-wires [4]. In eukaryotic algae, NADPH oxidase (NOX) is a potential candidate for plasma membrane electron transport. NOXs catalyse the reduction of extracellular O_2 into superoxide anions ($O_2^{\bullet-}$) utilising electrons from intracellular NADPH. NOX-generated superoxide is converted into other reactive oxygen species, which are important signalling molecules involved in many processes such as growth, development and stress signalling [7–10].

* Corresponding author.
E-mail addresses: anuphon.laohavisit@riken.jp (A. Laohavisit), aa612@cam.ac.uk (A. Anderson), pb346@cam.ac.uk (P. Bombelli), matt.jacobs@bristol.ac.uk (M. Jacobs), ch26@cam.ac.uk (C.J. Howe), jmd32@cam.ac.uk (J.M. Davies), as25@cam.ac.uk (A.G. Smith).
[1] Current address: RIKEN Centre for Sustainable Resource Sciences, 1-7-22 Suehiro, Tsurumi, Yokohama, Kanagawa 230-0045, Japan.
[2] Current address: Department of Physiology, Downing Site, University of Cambridge, CB2 3EG, UK.
[3] Current address: School of Biological Sciences, University of Bristol, Woodland Road, Bristol BS8 1UG, UK.

http://dx.doi.org/10.1016/j.algal.2015.08.009

NOXs have been identified in several algal species [11], and in many cases the production of superoxide anion is important for responses to biotic challenges. For example, in the heterokont *Chatonella marina* NOX-sourced superoxide anion is a defence response against fish grazing, as well as being essential for cell growth [12]. Superoxide anions have also been linked to a defence response in red algae [13], and in mediating interaction between dinoflagellates and their coral symbionts [14]. In marine diatoms, NOXs have been shown to be important in iron reduction and bioavailability [15], and in the green alga *Chlamydomonas reinhardtii*, NOXs are believed to be involved in mediating autophagy and responses to anaerobiosis [16,17]. Crucially, NOX proteins are electrogenic and have been implicitly linked to power output in biofuel cells [18,19]. As such they are excellent candidate proteins for improving BPV function.

Previous work in our laboratories has shown that *NOX* deletion in *C. reinhardtii* impairs superoxide anion production and BPV power output [20]. Complementation restores both superoxide anion production and BPV power output, confirming the role that NOXs play as crucial electron exporters. However, the real-world applicability of BPV devices will be limited by their power output, and the molecular approach with *C. reinhardtii* did not result in any increase in BPV performance. We therefore decided to approach the problem from a different perspective. Superoxide anion production can vary significantly depending on algal species [21] and production has been shown to be closely linked to growth phases in certain algae [12]. Species selection and growth regime are thus two obvious factors to investigate. Diatom species are excellent candidates for investigating this further, as they have long growth cycles that are readily amenable to manipulation. *Phaeodactylum tricornutum* and *Thalassiosira pseudonana* are two diatoms, phylogenetically very distant from *C. reinhardtii.* Both harbour two putative NOX genes in their genomes [11], and the predicted proteins are structurally diverse from all other NOX [13]. Specifically, they have additional transmembrane-domains and lack any calcium-regulatory mechanisms characteristic of human and plant NOXs [13], hence it was of physiological interest to investigate if such NOX would also be functional. Superoxide anion production has previously been recorded in *T. pseudonana* and is implicated in reduction of extracellular iron prior to uptake [15]. Additionally, in real-life BPV applications where temperature and light quality may change rapidly, it is essential to incorporate species that are durable to such fluctuations. Unlike many green algal species, diatoms, such as *P. tricornutum*, can withstand significant environmental changes in light wavelengths, temperature, salinity and availability of silicon [22], which are favourable attributes for BPV candidate species. Here, we have investigated NOX activity in these two diatom species, testing whether superoxide production is dynamic throughout growth in the diatoms, and if we can manipulate this to optimise power output in a BPV device.

2. Methods

2.1. Algal cultures, growth conditions and chemicals

P. tricornutum (strain 1055/1) and *T. pseudonana* (strain 1085/12) were obtained from the Culture Collection of Algae and Protozoa (CCAP) stock centre (CCAP, Oban, UK). *P. tricornutum* and *T. pseudonana* were grown in f/2 medium [37], using sea salts (Sigma, UK; catalogue number S9883) to make artificial sea water (35 g per litre for *P. tricornutum* and 31 g per litre for *T. pseudonana*). Cultures were grown in either diurnal (LD) light regime (16 h light:8 h dark) or continuous light (LL) regime with similar temperature and light intensity (23–25 °C, 40–50 $\mu E \cdot m^{-2} \cdot s^{-1}$, shaking at 150 rpm). Cells from a stationary phase culture were washed and used to re-inoculate fresh medium for experimental cultures at a known final cell density (determined by haemocytometer). All chemicals were from Sigma, UK unless otherwise stated.

2.2. Cell count and chlorophyll determination

Cells were immobilised and stained by adding 5 μl of Lugol's iodine solution (0.1% (*w*/*v*) iodine in 2% (*w*/*v*) potassium iodide solution) per 100 μl culture and counted using a haemocytometer (Improved Neubauer model, Hawksley, UK) under a Nikon Optiphot microscope (Nikon, USA). Chlorophyll extraction was done according to the method of Inskeep and Bloom [38]. Cells were incubated in DMF (dimethylformamide; Fisher's Scientific, UK) in the dark for 24 h at 4 °C, centrifuged for 5 min at 13,000 rpm and the absorbance of the supernatant at A_{630} and A_{664} was recorded using a spectrophotometer (Helios Alpha, Thermo Scientific, UK). Total chlorophyll content was calculated as: Total Chlorophyll (mg L^{-1}) = $7.74 \cdot A_{664} + 23.39 \cdot A_{630}$.

2.3. Extracellular superoxide detection

Algal cultures at indicated stages of growth were harvested by centrifugation (3000 *g*, 10 min) and resuspended in Tris–HCl buffer (20 mM, pH 7). Cells were counted and an equal number of cells aliquoted into separate microfuge tubes. Cells were centrifuged again and resuspended in Tris–HCl buffer plus 200 μM (final concentration) XTT (2,3-bis-(2-methoxy-4-nitro-5-sulfophenyl)-2*H*-tetrazolium-5-carboxanilide). Samples were illuminated with white LED lights (OSRAM Parathom Par 16, OSRAM GmbH, Germany) at a light intensity of 60–70 $\mu E \cdot m^{-2} \cdot s^{-1}$, rotated continuously at 16 rpm and kept at a temperature of 22–24 °C. Cell aliquots were collected at indicated time points after light exposure, centrifuged (13,000 *g*, 1 min), and the absorbance (A_{470}) of the supernatant was measured with a plate reader (Fluostar Optima, BMG Labtech, USA). Cell pellets were kept for chlorophyll extraction as described above. Superoxide anion levels were quantified according the extinction coefficients described by [23]. For experiments in the dark, the cell samples were covered completely with black cloth for the duration of the experiment. For the experiment with DPI and DMSO, the cells were treated with DPI or equivalent concentration of DMSO during the wash steps, washed again with buffer to remove DPI or DMSO, and the experiment was carried out as normal.

2.4. Current determination with a BPV

BPV devices were formed from 10 mm thick transparent Perspex with a main circular anodic chamber of external diameter 50 mm, internal diameter 44 mm and 20 mm depth (nominal internal volume 30.6 ml and 15.3 cm^2 illuminated area) similar to the device described previously [3]. An 80 × 80 mm carbon-platinum cathode assembly impregnated on one side (50 × 50 mm coated area) with Nafion (Ion Power, USA) formed the back wall of the anodic chamber. A single layer of dialysis membrane (SnakeSkin Dialysis Tubing 10K MCWO, Sigma) was layered on to the cathode assembly (Nafion side). Transparent indium tin oxide (ITO, 60 Ω sq^{-1}) on plastic polyethylene terephthalate (Sigma, UK) formed the front of the anodic chamber. Junctions between Perspex layers were sealed with polydimethylsiloxane (PDMS) and held in place by bolts. Electrodes were attached to the external circuit with a crocodile clip via a contact formed from a strip of stainless steel. Current was monitored via a multimeter (Model UT70B, Uni-Trend, Hongkong) and recorded using UT70B interface software v3.04 (Uni-Trend, China). A bias potential (500 mV) was applied between the anode and cathode by means of an external power box made in house. The device was illuminated through the ITO side by a panel of red LED bulbs (maximum emission peak 630 nm) controlled by a PSU130 power unit (LASCAR, Salisbury, UK). Light intensity was set at 100 $\mu E \cdot m^{-2} \cdot s^{-1}$ measured by a quantum sensor (Q.LR, Skye Instruments, Powys, UK). Algal suspensions in medium were loaded directly into the device via a 4 mm hole in the top of the anodic chamber, which was plugged during operation to prevent evaporation. Potassium ferricyanide (FeCN) was added to a final concentration of 1 mM, XTT was added to a final concentration of 200 μM and cultures

were continuously mixed via a small magnetic stirrer within the anodic chamber controlled by a magnetic stirrer unit on setting 4 (Multistirrer 6, VELP Scientifica, Italy). The set-up was completely covered by black velvet fabric to ensure complete darkness. Devices were operated at room temperature (~21 °C). Dialysis membrane was replaced for each experiment and the other components washed with deionised water before re-use.

2.5. NOX transcript analysis

P. tricornutum cultures were grown under LL or LD light regime, harvested by centrifugation at 4 or 8 days postinoculation and frozen in liquid nitrogen. Cells were disrupted by vortexing with 300 mg glass beads (425–600 μm, Sigma-Aldrich, UK) for 10 min in 0.5 ml lysis buffer (20 mM Tris–HCl pH 8.0, 20 mM EDTA, 5% (*v*/*v*) SDS). Total RNA was extracted from lysed cells using the Qiagen RNeasy Plant Mini Kit (Qiagen, UK), followed by treatment with Ambion Turbo DNase-Free Kit (Invitrogen, UK) to remove genomic DNA. RNA was reverse-transcribed into cDNA with Superscript III (Invitrogen, UK). Quantitative PCR was carried using Qiagen SYBR Green MasterMix (Qiagen, UK) on a Qiagen Rotor-Gene Q instrument, using 5 ng cDNA and 0.1 μM of each primer per reaction. Cycling conditions were: 95 °C for 10 min, followed by 40 cycles of 95 °C for 5 s and 65 °C for 15 s. Unique single products were verified by melt curve analysis. No amplification was detected in RT-minus samples confirming complete removal of genomic DNA. Cycle threshold (Ct) values of two technical replicates were calculated using Rotor-Gene Q Software V.2.02 (Qiagen, UK) and the mean reaction efficiency (within ±5% of the median efficiency) of each primer pair was quantified using LinReg PCR software [39]. Quantification of targets was based on the Pfaffl model (Efficiency$^{-Ct\ target}$; [40]). Levels of target amplicons were normalised to the mean RE$^{-Ct\ endogenous\ controls}$ (*H4*, *RPS* and *TBP*; [41]) and calculated by dividing the normalised expression values. Primers used in qPCR are listed in Supplementary Table 1.

3. Results

3.1. Superoxide production by diatoms varies during growth

Previous research has shown that *T. pseudonana* can generate superoxide anions [15], so we investigated NOX activity at different stages of growth to understand further the dynamics of superoxide anion production by diatoms. Cell cultures were grown under continuous light (LL), and growth of both species showed expected patterns of exponential and stationary growth phases. Two logarithmic growth phases (primary and secondary, Log1 and Log2), a stationary growth phase, and a lag phase (for *P. tricornutum*) were identified (Fig. 1A and B). We used a cell-impermeable reporter (XTT; 2,3-bis-(2-methoxy-4-nitro-5-sulfophenyl)-2H-tetrazolium-5-carboxanilide [23]) to measure extracellular superoxide anion production as an indicator of NOX activity, and assayed cell samples at indicated days of growth for 120 min, normalising superoxide anion production to cell number. Maximum superoxide anion production corresponded with the primary growth phase of *P. tricornutum*, and the secondary growth phase for *T. pseudonana*. *P. tricornutum* superoxide anion production declined from Day 4, greatly decreasing on Day 5, and continued to decline until Day 11 (Fig. 1A). For *T. pseudonana*, superoxide production was low until Day 5, after which production increased and reached its highest level on Day 7, then began to decrease (Fig. 1B), and generated 2-fold higher superoxide levels per cell than *P. tricornutum*. To gain more insight into the potential role of superoxide in the growth of *P. tricornutum* and *T. pseudonana*,

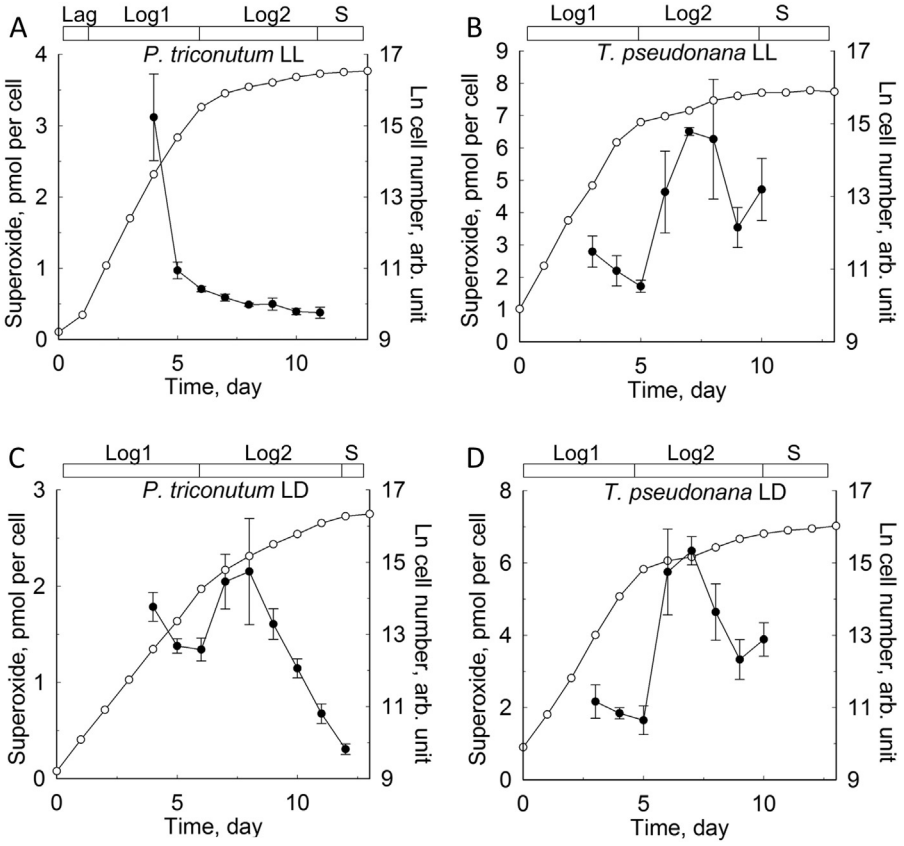

Fig. 1. Light regime influences diatom growth and thus extracellular superoxide production in *P. tricornutum* but not *T. pseudonana*. Growth (empty circles, plotted as a logarithmic (ln) function of total cell number) and superoxide anion production (filled circles) of *P. tricornutum* and *T. pseudonana* cultures grown in f/2 medium in constant (LL) light (A–B) and diurnal (LD) light (C–D). Bars above graphs indicate growth phases (S, stationary phase). Data are mean ± SEM (n = 3).

both species were grown under diurnal light (LD). There was no effect of light regime on growth of *T. pseudonana* (Fig. 1D), but growth of *P. tricornutum* was slower under LD light compared to LL light (Fig. 1C). Similarly, the pattern of superoxide anion production by LD-grown *P. tricornutum* was very different from LL-grown cells. Levels were high on Day 4, then declined between Days 5 and 6 and subsequently increased. *P. tricornutum* cells produced most superoxide anion on Day 8 at levels similar to that of Day 4, and after Day 8, production decreased progressively per day. When the ln-transformed growth curve was superimposed onto superoxide anion production, high production still coincided with the primary log phase at Day 4, but also matched the secondary log phase at Day 8.

Superoxide anion production patterns for LD-grown *T. pseudonana* showed no difference from LL-grown cells, reaching their highest point at the secondary logarithmic growth phase (Fig. 1B and D). Comparing LL- and LD-grown *P. tricornutum* cells, Day 4 LL-grown cells generated higher superoxide anion levels, but subsequently more was produced by LD-grown cells than LL-grown cells between Day 5 and Day 11, with the clearest difference seen on Day 8 (Fig. 1C). In summary, diatom superoxide anion production was dynamic throughout growth, and maximum production coincided with the secondary logarithmic growth phases, whilst low superoxide reflected the stationary growth phase.

Given that the biogenesis of silicified frustules is facultative for *P. tricornutum* [24], we tested whether growing cells in the absence of silicon would affect cell growth and thus superoxide anion production. Cultures without silicon in the medium showed no difference in growth compared with cultures supplemented with silicon in both LL and LD regimes (Supplementary Fig. 1). This was reflected in superoxide anion production as there was no difference between cultures with or without silicon for LD or for LL regime.

3.2. Characterisation of NOX activity in P. tricornutum

Our results so far suggested that a functional NOX was present in both *P. tricornutum* and *T. pseudonana*. To test this, we used a pharmacological approach. NOX is inhibited by diphenyleneiodonium chloride (DPI) and this inhibitor is widely used to establish NOX activity [25]. Superoxide anion production was significantly lower in both LD- and LL-grown, DPI-treated cells compared to the control after 120 min ($p = 0.0018$, LD-grown; $p = 0.032$, LL-grown; Student's *t*-test; Fig. 2). Dimethylsulphoxide (DMSO) was used as used as a carrier for DPI and no difference was observed in superoxide anion production between cells exposed to the equivalent concentration of DMSO alone and the control (Fig. 2). Overall, the data demonstrated that DPI treatment completely abolished superoxide production.

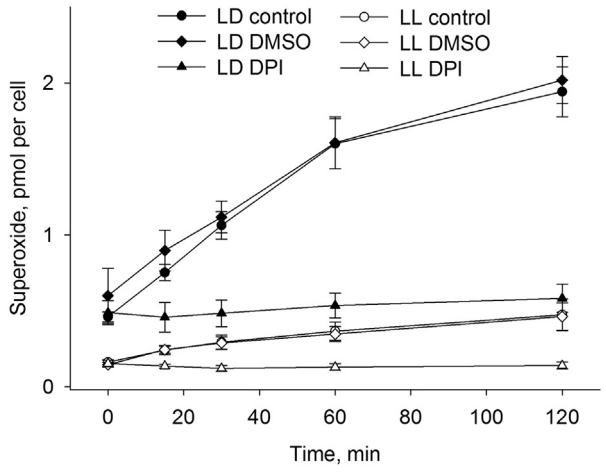

Fig. 2. NOX-inhibitor diphenyleneiodonium chloride (DPI) strongly inhibits superoxide anion production. *P. tricornutum* cells were grown for 8 days in LD or LL regime, incubated with 20 μM DPI for 1 h and assayed for superoxide anion in the presence of 20 μM DPI for 120 min. Separate controls with equivalent DMSO concentration (0.06% *v*/*v*) are shown. Data are mean ± SEM (n = 3).

Previous work has shown that because electrons are sourced from the light reactions of photosynthesis, power generation within BPV devices is light-stimulated [3]. NOXs transfer electrons from cytosolic NADPH, which in plants is likely to be derived from photosynthetic reactions [26]. Therefore, to examine if the NOX-sourced superoxide anion production in *P. tricornutum* was light dependent, 8-day old LL- and LD-grown cells were assayed in the light or in the dark. Superoxide anion production was light-dependent in both LL- and LD-grown cultures (Fig. 3A). Illumination markedly increased superoxide anion generation in both LD-grown cells ($p = 0.02$; Student's *t*-test) and LL-grown cells ($p = 0.0001$; Student's *t*-test) compared to dark, though to a lesser extent in LL-grown cells. A similar effect was observed in LD and LL cells grown with Si in the medium (Supplementary Fig. 2). Altogether, the data indicate that superoxide anion production is dependent upon light.

BPV current output has been shown previously to correlate with cell chlorophyll content [3]. We measured chlorophyll in *P. tricornutum* cells grown in LD and LL regimes (Fig. 3B). Initially, chlorophyll content was greater in LL-grown cells compared to LD-grown cells, but LD-grown cells contained a similar amount of chlorophyll on Day 8 (Supplementary

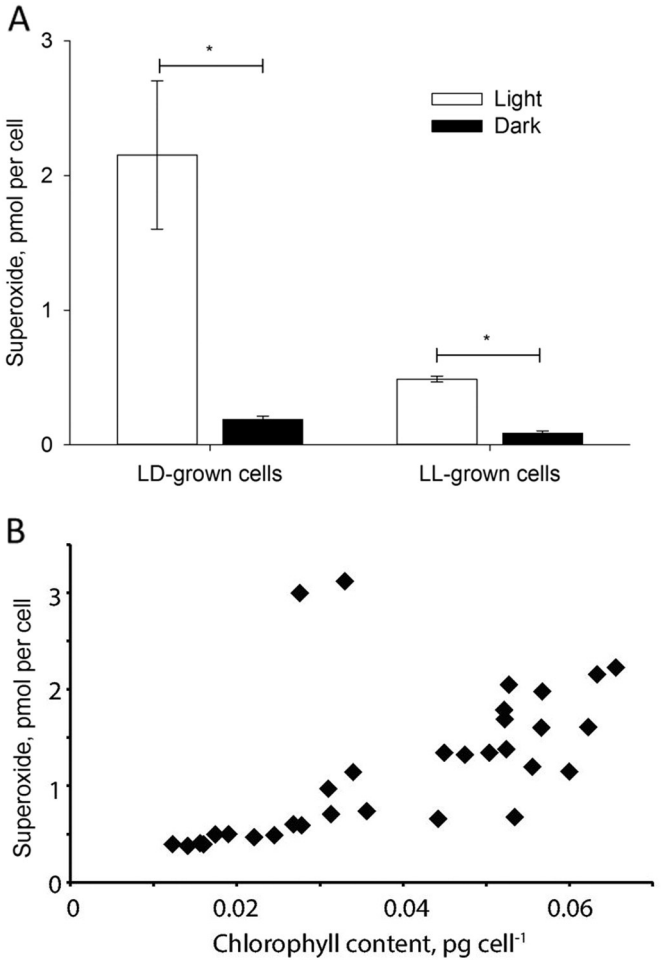

Fig. 3. Light and chlorophyll content are important for superoxide anion production. A, Superoxide anion production is light dependent. *P. tricornutum* cells were grown for 8 days in different light regimes (LD or LL) and assayed for 120 min either in light or in the dark. Data are mean ± SEM ($n = 3$). Significances (*$p < 0.05$) in B were determined by Student's *t*-test. B, Superoxide production is positively correlated with chlorophyll content per cell. Cells were harvested between Days 4 and 13.

Fig. 3). Chlorophyll production in LD-grown cells increased until Day 12, whilst in LL-grown cells, the chlorophyll content started decreasing after Day 8. The relationship between superoxide anion production and chlorophyll content per cells was positively correlated with an R^2 value of 0.31 (Fig. 3B).

3.3. Relating BPV current output to superoxide production

We investigated if superoxide anion production would correlate with current generation, and thus power output, by measuring the steady-state currents generated by the diatoms in a BPV device [3]. The BPV device and principles of operation are displayed in Supplementary Fig. 4. Given the rate of superoxide production (2 pmol superoxide per cell per 120 min) shown in Fig. 3, the expected current output could reach up to 26.8 $pA \cdot cell^{-1}$ (2.68 $A \cdot m^{-2}$ and 134.4 $A \cdot m^{-3}$). *P. tricornutum* cells were grown in LD or LL regime for 8 days and were tested for current generation using the BPV device, in which a bias potential of 500 mV was applied to allow effective measurement of current output, and thus electrogenic potential of the algae. Current output increased when the device was illuminated, eventually reaching a steady-state current. Steady currents can be quantified as shown on representative graphs for each diatom species (Fig. 4). LD-grown *P. tricornutum* cells had a significantly higher mean steady-state dark current (following the end of illumination; $p = 0.0019$; Student's *t*-test) and steady-state light current ($p = 0.017$; Student's *t*-test) than LL-grown cells (Fig. 4B). In addition, steady-state currents were greater during illumination compared to during the following dark period, which would be expected if power output were related to superoxide

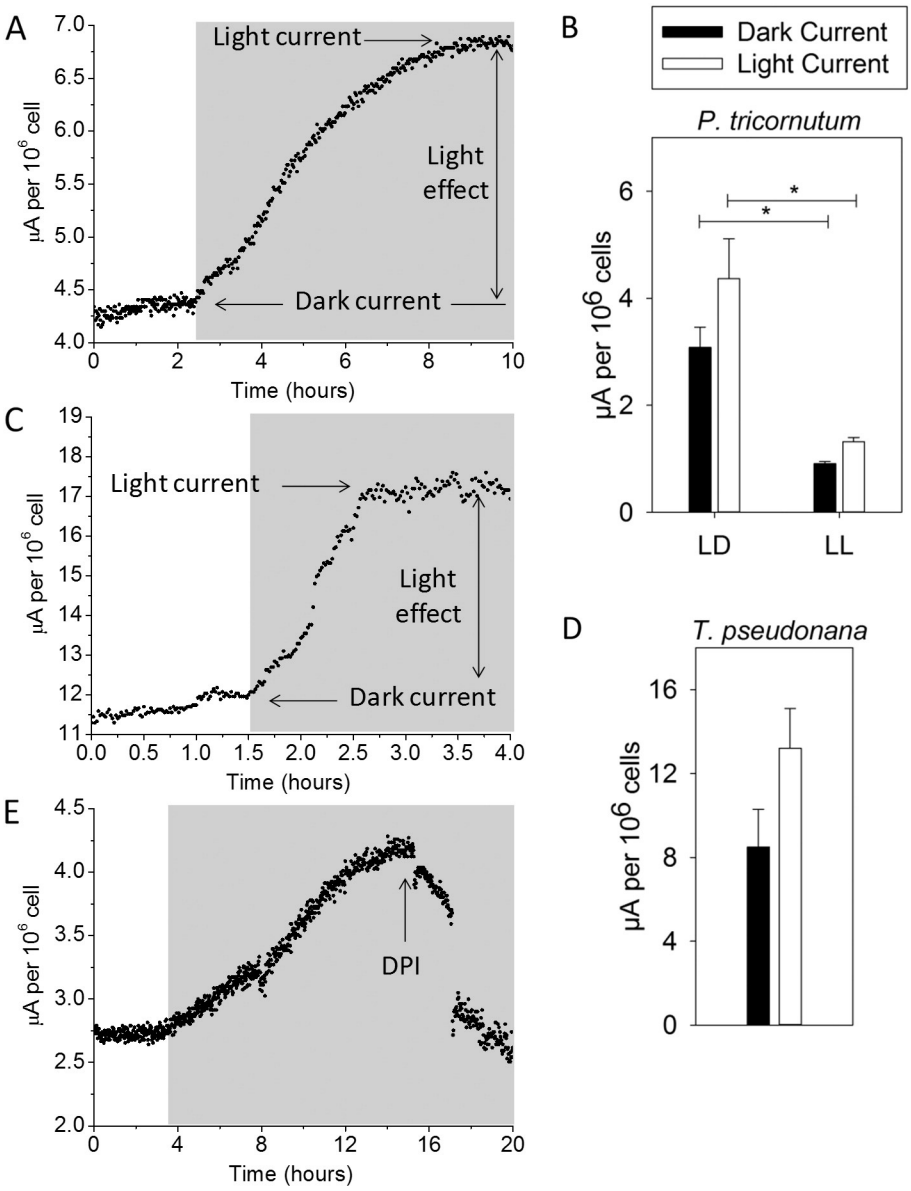

Fig. 4. Current output in a BPV device is light-, growth- and species-dependent and relates to NOX-sourced superoxide anion production. A, Representative trace of current generation by 8 day old LD-grown *P. tricornutum* cells in a BPV device to which a bias potential of 500 mV was applied. Cells were adapted to the dark before being illuminated (grey boxes) and allowed to reach a steady-state 'light current'. Lights were then switched off and current allowed to reach a steady-state 'dark current'. This was done twice in each experiment and the steady light and dark currents quantified (indicated). B, Mean light and dark currents for 8 day old LD- and LL-grown *P. tricornutum*. C, Representative trace of the current generation by LD-grown *T. pseudonana* cells in the BPV device. The experimental set up is the same as A. D, Mean light and dark currents for LD-grown *T. pseudonana*. E, DPI inhibited current generation in 8 day old LD-grown *P. tricornutum*. The experimental setup is the same as A. DMSO (0.06% *v*/*v*) and DPI (20 μM final concentration) were added at indicated times. All data are presented as microamperes (μA) per 10^6 cells. Significances (*$p < 0.05$) in B were determined by Student's *t*-test. Data are mean ± SEM ($n = 3$–6, with the exception of E where $n = 1$).

anion production, which is also light dependent (Fig. 3A). Power output therefore mirrored the superoxide anion production capabilities of LD- and LL-grown *P. tricornutum* (Fig. 1).

T. pseudonana showed similar light-dependent current output in the BPV device (Fig. 4C) and the quantified currents were considerably greater than those of *P. tricornutum* (Fig. 4D). *T. pseudonana* also had greater superoxide anion production than *P. tricornutum* (Fig. 1) and overall, the data suggest that superoxide anion production is positively correlated with current generation by diatoms.

To test if current output were due to NOX activity, DPI was added to a *P. tricornutum* LD-grown culture in the BPV device. Addition of 20 μM DPI immediately caused current reduction in the light phase (Fig. 4E). Current dropped from about 4 μA to about 2 μA and did not drop further upon ceasing illumination (Fig. 4B), whereas no effect was seen after addition of DMSO, and a light-induced current increase was still recorded (data not shown). Therefore, it appears that a significant amount of the current output in the BPV device is likely due to NOX activity.

3.4. Expression of NOX genes is regulated by light exposure

Expression of the putative *P. tricornutum* NOX genes was examined to test for a link between the difference in superoxide anion production and power output by LD- and LL-grown *P. tricornutum*. Given that the *P. tricornutum* LL- and LD-grown cells are isogenic, we could compare the transcriptional changes between the two cultures directly. *P. tricornutum* is known to contain two putative NOX genes, *PtNOX1* and *PtNOX2* [11,13]. Quantitative Reverse-Transcription PCR (qRT-PCR) was carried out to investigate their expression in cells grown under LD or LL regime at Day 4 and Day 8 of growth (Fig. 1). Transcript level of *PtNOX1* was significantly greater in LL-grown cultures than LD-grown cultures at Day 4, and significantly greater in LD-grown cultures than LL-cultures at Day 8 (Fig. 5). Expression of *PtNOX1* increased significantly between Day 4 and Day 8 for LD-grown cells, though remained unchanged in LL-grown cells. For *PtNOX2*, transcript level was greater in LL-grown cells than LD-grown cells at Day 4 and no difference in expression was seen between LL- and LD-grown cells at Day 8. *PtNOX2* increased between Day 4 and Day 8 in both LL- and LD-grown cells. Examining each day individually, *PtNOX1* expression reflected the patterns of superoxide anion production (Fig. 1), and the significantly higher expression of *PtNOX1* in LD cultures at Day 8 corresponds to increased power output of LD cultures (Fig. 4B).

3.5. Semi-continuous P. tricornutum culturing maintains high production of superoxide anion

Although at Day 8 of growth, LD-grown *P. tricornutum* cultures showed the highest superoxide anion production it decreased soon after (Fig. 1C). Given the correlation between superoxide anion production and current generation, it would be desirable to maintain this superoxide anion production at its maximum, ensuring high power output. Semi-continuous cultures were used to investigate if superoxide anion production could be sustained if cultures were maintained at 'Day 8' equivalent cell number. LD- and LL-grown cells were grown to stationary phase (Day 10 equivalent cell number) and used to re-inoculate to Day 6 equivalent cell number. Cells were grown for two days to Day 8 equivalent cell number and superoxide anion production was measured. Remaining cultures were allowed to grow to Day 10 again and the experiment was repeated twice (i.e., up to three generations). Semi-continuous LD-grown cultures produced equivalent levels of superoxide anion production at 120 min to the batch LD-grown culture (Fig. 6). Semi-continuous LD-grown cultures also showed a greater superoxide anion production than semi-continuous LL-grown cultures ($p = 0.007$; Student's *t*-test). It may therefore be possible to maintain high current generation by utilising a semi-continuous culturing technique.

4. Discussion

Here we have shown that two marine diatoms, *P. tricornutum* and *T. pseudonana*, generate extracellular superoxide anion, and that this correlates with their ability to generate current in a BPV device. Production of superoxide by *P. tricornutum* was completely abolished by DPI (Fig. 2), diagnostic of NOX activity [25,27] and by similar DPI concentrations used to inhibit production of reactive oxygen species by other algae [28]. *T. pseudonana* superoxide production has been recorded previously [15], but we believe that this is the first experimental evidence of NOX activity in *P. tricornutum*, supporting the presence of NOX gene sequences [11,13]. Transcript analysis indicated that in *P. tricornutum*,

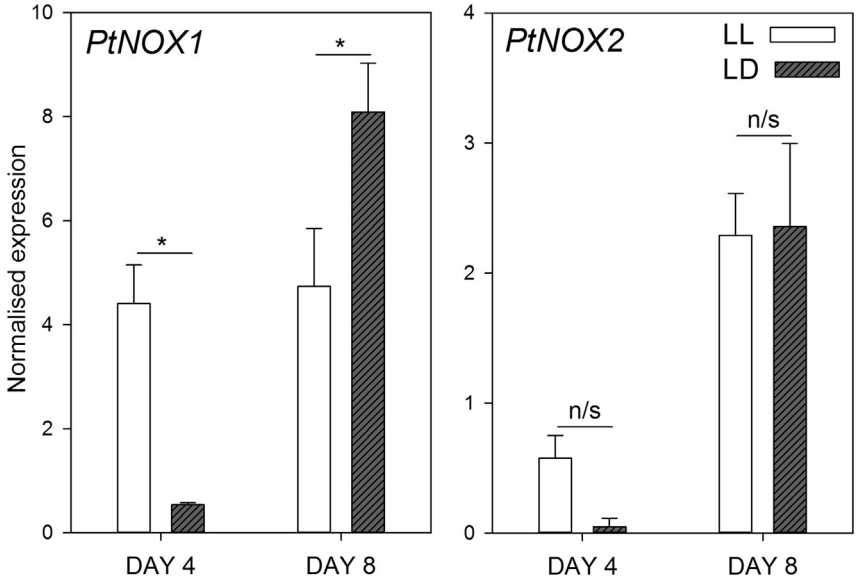

Fig. 5. Expression of *PtNOX1* and *PtNOX2* in *P. tricornutum* cells. Cultures were grown in diurnal (LD) or continuous (LL) light regime and harvested at Day 4 or Day 8 of growth post-inoculation. qRT-PCR was conducted as described in Methods. Primers are listed in Additional Table 1. Expression was normalised to the mean expression of reference genes *H4*, *RPS* and *TBP*. Significance was determined with One-Way ANOVA (*$p < 0.05$); n/s, no significance. Data are mean ± SEM ($n = 4$).

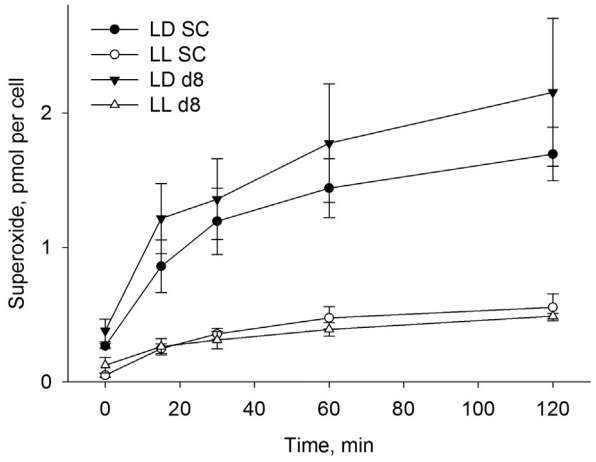

Fig. 6. Quantitative measurement of superoxide anion for 8 days old *P. tricornutum* semi-continuous and batch cultures in the presence of Si. Cultures were assayed at Day 8 (d8) and subsequently at semi-continuous "Day 8" (SC; see text and Methods for more details). Superoxide anion was measured at an assay time-point of 120 min and normalised to cell number. Data are mean ± SEM ($n = 3$).

PtNOX1 may play the key role in superoxide generation (Fig. 5), although *PtNOX2* may be constitutively expressed, regardless of light regime. Higher levels of superoxide anion production by *T. pseudonana* compared with *P. tricornutum* were also matched by greater current generation in the BPV device by *T. pseudonana* (Fig. 4). Additionally, the diminution of current output in the BPV device by DPI (Fig. 4E) confirms our hypothesis that NOX is a key component of electron efflux from the diatom in BPV devices.

Importantly, our findings support our previous observations in the green alga *C. reinhardtii* [20] and are consistent with previous reports on human cells, where NOX inhibitors abolished electrical current in isolated phagocytes [18], and inhibited current output by macrophages in biofuel cells [19]. Strikingly, diatoms generate much higher currents than animal cells. The current obtained with macrophages was 1.5–2 μA per 10^6 cells, whilst *T. pseudonana* generated 14 μA per 10^6 cells (Fig. 4C), which is equivalent to 140 μA per mL of culture. With *C. reinhardtii*, currents of ~75 μA per 10^6 cells were recorded, and normalising for lower cell density means that this corresponds to 12 μA per mL culture [20]. At present, a current output of around 50 mA m^{-2} has been observed when a BPV device was operated with a sessile film of the marine cyanobacterium *Synechococcus* sp. WH 5701 [5]. When the unicellular green alga *Chlorella vulgaris* was exploited in a planktonic device, with only ferricyanide as the extracellular electron carrier, around 110 mA m^{-2} was observed [29]. Given the rate of superoxide production by diatoms, we would expect a current output of ca. 536 mA m^{-2}, a figure that substantially surpasses these previously published reports. As NOX genes are evident in a range of algal genomes [11], and given the enormous diversity in the algal kingdom, it is likely that other diatom species may generate even higher current. The use of diatoms therefore raises the prospect of enhanced power output, with NOX and extracellular superoxide anion production as desirable attributes for microbes used in BPV devices.

Simple alterations of the light regime for *P. tricornutum* induced higher superoxide anion production and power output. We would envisage BPV devices being used outdoors (i.e., under diurnal conditions), therefore it is promising that *P. tricornutum* generated a higher current under the LD regime than LL. Furthermore, the ability of *P. tricornutum* to function similarly in BPVs in the presence or absence of Si indicates possibilities of operation in both lab and natural conditions [22]. Since superoxide anion production varies throughout the growth cycle of *P. tricornutum* in batch culture, with the highest level corresponding to the exponential phase of growth (Fig. 1), we reasoned that we could sustain constant high levels of superoxide anion production by 'semi-continuous' growth, where cells are maintained in an actively-growing state. Indeed this is what we observed (Fig. 6). Our demonstration that we can maintain high superoxide production by growing cells in a 'semi-continuous' culture (Fig. 6), is a novel, cost-effective and simple method of ensuring maximal power output, that requires no transgenic strains. In larger scale BPV devices, this could be achieved by implementing a medium-flushing and re-feeding system, maintaining cultures at 'day 8' (for example) equivalent cell number. Superoxide is clearly linked to growth stages in diatoms (Fig. 1) and other algae [30] and lowering cell density to 'day 8' equivalent likely re-initiates cell proliferation. NOX activity and superoxide anion production are known to support growth of plant cells [25] and growth of *C. marina* was abolished by superoxide dismutase, linking superoxide anion production with cell proliferation [30]. *P. tricornutum* and *T. pseudonana* showed dynamic superoxide anion production throughout growth, peaking during exponential phase (Fig. 1). Dynamic patterns of superoxide anion production during the growth cycle have also been reported in *C. antiqua* [12], which also showed maximal superoxide anion production during the exponential phase of growth. We propose that assaying NOX or BPV activity throughout the growth cycle should be the focus of future studies on BPV, and other fuel cell, performance.

Further improvements in BPV output may come from understanding the biological basis of NOX activity in diatoms. Superoxide anion production has been recorded in numerous algae and is implicated in promoting growth and responses to environmental stress, predators and pathogens [30–32]. Reported levels of production of superoxide anion vary between algal species, ranging from about 0.1 pmol $cell^{-1}$ in *C. antiqua* [12] to 14.4 pmol $cell^{-1}$ in *C. marina* [33]. *P. tricornutum* and *T. pseudonana* produced around 3–7 pmol superoxide $cell^{-1}$, which is appreciably higher than most other surveyed algal species [34] and could point to a possibly important role in cellular function. *T. pseudonana* reduces extracellular Fe^{3+} via generation of extracellular superoxide anion to enable uptake [15], but most of the Fe^{2+} is rapidly re-oxidised to Fe^{3+}, necessitating increased generation of superoxide anion, which may explain why *T. pseudonana* produces such high superoxide levels. Conversely, *P. tricornutum* possesses transmembrane ferric-reductase enzymes which are upregulated under iron starvation [35] so the precise role of superoxide remains unclear. However, both *P. tricornutum* and *T. pseudonana* can grow in Fe-limited medium and it is possible that this would enhance superoxide anion production for BPV power output by increasing superoxide, or activation of other transmembrane iron-reduction components.

In conclusion, we have demonstrated a link in diatoms between NOX-sourced superoxide anion and power output in BPV devices. The residual current and superoxide anion generation in the presence of DPI show that there are electron export mechanisms that remain to be identified and exploited. Superoxide anion-generating apoplastic peroxidases have been found in *Arabidopsis thaliana*, where they are involved in the oxidative burst in response to pathogen attack [36] and there may be equivalents in algae. Nonetheless, testing algal strains for high NOX activity is a straightforward selection step for high-current generating strains suitable for use in BPV devices, using the colorimetric assay we describe here. Commercialised BPVs would likely need to operate in a multitude of environments, therefore our demonstration that diatom-based BPVs are durable (e.g. under varying light regimes, cell growth stages and presence or absence of Si) and are of higher-performance than equivalent BPVs, supports the potential feasibility of diatom-based BPV operations.

Competing interests

The authors declare no competing interests.

Authors' contributions

AL performed growth experiments, NOX activity measurements and BPV experiments; AA conducted qRT-PCR experiments; PB conducted BPV experiments; MJ carried out growth and NOX activity experiments; AL, AA, and PB analysed the data and wrote the manuscript; CJH, JMD and AGS conceived the study, interpreted experimental data and wrote the manuscript.

Acknowledgements

This work was supported by the United Kingdom Engineering and Physical Sciences Research Council (EPSRC), grant reference EP/F047940/1.

Appendix A. Supplementary data

Supplementary data to this article can be found online at http://dx.doi.org/10.1016/j.algal.2015.08.009.

References

[1] N.S. Lewis, D.G. Nocera, Powering the planet: chemical challenges in solar energy utilization, Proc. Natl. Acad. Sci. U. S. A. 103 (2006) 15729–15735.
[2] M. Rosenbaum, Z. He, L.T. Angenent, Light energy to bioelectricity: photosynthetic microbial fuel cells, Curr. Opin. Biotechnol. 21 (2010) 259–264.
[3] P. Bombelli, R.W. Bradley, A.M. Scott, A.J. Philips, A.J. McCormick, S.M. Cruz, A. Anderson, K. Yunus, D.S. Bendall, P.J. Cameron, J.M. Davies, A.G. Smith, C.J. Howe, A.C. Fisher, Quantitative analysis of the factors limiting solar power transduction by *Synechocystis* sp. PCC6803 in biological photovoltaic devices, Energy Environ. Sci. 4 (2011) 4690–4698.
[4] R.W. Bradley, P. Bombelli, S.J.L. Rowden, C.J. Howe, Biological photovoltaics: intra- and extra-cellular electron transport by cyanobacteria, Biochem. Soc. Trans. 40 (2012) 1302–1307.
[5] A.J. McCormick, P. Bombelli, A.M. Scott, A.J. Philips, A.G. Smith, A.C. Fisher, C.J. Howe, Photosynthetic biofilms in pure culture harness solar energy in a mediatorless bio-photovoltaic cell (BPV) system, Energy Environ. Sci. 4 (2011) 4699.
[6] P. Bombelli, T. Müller, T.W. Herling, C.J. Howe, T.P.J. Knowles, A high power-density, mediator-free, microfluidic biophotovoltaic device for cyanobacterial cells, Adv. Energy Mater. 1401299 (2014).
[7] R. Mittler, S. Vanderauwera, N. Suzuki, G. Miller, V.B. Tognetti, K. Vandepoele, M. Gollery, V. Shulaev, F. van Breusegem, ROS signaling: the new wave? Trends Plant Sci. 6 (2011) 300–309.
[8] B. Kawahara, M.T. Quinn, J.D. Lambeth, Molecular evolution of the reactive oxygen-generating NADPH oxidase (Nox/Duox) family of enzymes, BMC Evol. Biol. 7 (2007) 109.
[9] J. Aguirre, J.D. Lambeth, Nox enzymes from fungus to fly to fish and what they tell us about Nox function in mammals, Free Radic. Biol. Med. 49 (2010) 1342–1353.
[10] D. Marino, C. Dunand, A. Puppo, N. Pauly, A burst of plant NADPH oxidases, Trends Plant Sci. 17 (2012) 9–15.
[11] A. Anderson, J.H. Bothwell, A. Laohavisit, A.G. Smith, J.M. Davies, NOX or not? Evidence for algal NADPH oxidases, Trends Plant Sci. 16 (2011) 579–581.
[12] D. Kim, M. Watanabe, Y. Nakayasu, K. Kohata, Production of superoxide anion and hydrogen peroxide associated with cell growth of *Chattonella antiqua*, Aquat. Microb. Ecol. 35 (2004) 57–64.
[13] C. Hervé, T. Tonon, J. Collén, E. Corre, C. Boyen, NADPH oxidase in eukaryotes: red algae provide new hints! Curr. Genet. 49 (2005) 190–204.
[14] E. Saragosti, D. Tchernov, A. Katsir, Y. Shaked, Extracellular production and degradation of superoxide in the coral stylophora pistillata and cultured Symbiodinium, PLoS One 5 (2010) e12508.
[15] A.B. Kustka, Y. Shaked, A.J. Milligan, D.W. King, F.M.M. Morel, Extracellular production of superoxide by marine diatoms: contrasting effects on iron redox chemistry and bioavailability, Limnol. Oceanogr. 50 (2005) 1172–1180.
[16] M.E. Pérez-Pérez, I. Couso, J.L. Crespo, Carotenoid deficiency triggers autophagy in the model green alga *Chlamydomonas reinhardtii*, Autophagy 8 (2012) 376–388.
[17] A. Hemschemeier, D. Casero, B. Liu, C. Benning, M. Pellegrini, T. Happe, S.S. Merchant, Copper response regulator1-dependent and -independent responses of the *Chlamydomonas reinhardtii* transcriptome to dark anoxia, Plant Cell 25 (2013) 3186–3211.
[18] J. Schrenzel, L. Serrander, B. Bánfi, O. Nüsse, R. Fouyouzi, D.P. Lew, N. Demaurex, K.H. Krause, Electron currents generated by the human phagocyte NADPH oxidase, Nature 392 (1998) 734–737.
[19] M. Sakai, A. Vonderheit, X. Wei, C. Kuttel, A. Stemmer, A novel biofuel cell harvesting energy from activated human macrophages, Biosens. Bioelectron. 25 (2009) 68–75.
[20] A. Anderson, A. Laohavisit, I.K. Blaby, P. Bombelli, C.J. Howe, S.S. Merchant, J.M. Davies, A.G. Smith, Exploiting algal NADPH oxidase for biophotovoltaic energy, Plant Biotechnol. J. (2015)http://dx.doi.org/10.1111/pbi.12332.
[21] J.-A. Marshall, M. Hovenden, T. Oda, G.M. Hallegraeff, Photosynthesis does influence superoxide production in the ichthyotoxic alga *Chattonella marina* (Raphidophyceae), J. Plankton Res. 24 (2002) 1231–1236.
[22] P. Zhao, W. Gu, S. Wu, A. Huang, L. He, X. Xie, S. Gao, B. Zhang, J. Niu, A.P. Lin, G. Wang, Silicon enhances the growth of *Phaeodactylum tricornutum* Bohlin under green light and low temperature, Sci. Rep. 4 (2014) 3958.
[23] M.W. Sutherland, B.A. Learmonth, The tetrazolium dyes MTS and XTT prodvide new quantitative assays for superoxide and superoxide dismutase, Free Radic. Res. 27 (1997) 283–289.
[24] C. Bowler, A. De Martino, A. Falciatore, Diatom cell division in an environmental context, Curr. Opin. Plant Biol. 2010 (13) (2010) 623–630.
[25] J. Foreman, V. Demidchik, J.H.F. Bothwell, P. Mylona, H. Miedema, M.A. Torresk, P. Linstead, S. Costa, C. Brownlee, J.D.G. Jones, J.M. Davies, L. Dolan, Reactive oxygen species produced by NADPH oxidase regulate plant cell growth, Nature 422 (2003) 442e446.
[26] R. Scheibe, Malate valves to balance cellular energy supply, Physiol. Plant. 120 (2004) 21–26.
[27] F.F. Simon-Plas, T. Elmayan, J.-P. Blein, The plasma membrane oxidase NtrbohD is responsible for AOS production in elicited tobacco cells, Plant J. 31 (2002) 137–147.
[28] C. Ross, F.C. Küpper, V. Vreeland, J. Herbert Waite, R.S. Jacobs, Evidence of a latent oxidative burst in relation to wound repair in the giant unicellular chlorophyte *Dasycladus vermicularis*, J. Phycol. 41 (2005) 531–541.
[29] P. Bombelli, M. Zarrouati, R.J. Thorne, K. Schneider, S.J.L. Rowden, A. Ali, K. Yunus, P.J. Cameron, A.C. Fisher, D. Ian Wilson, C.J. Howe, A.J. McCormick, Surface morphology and surface energy of anode materials influence power outputs in a multi-channel mediatorless bio-photovoltaic (BPV) system, Phys. Chem. Chem. Phys. 14 (2012) 12221–12229.
[30] T. Oda, J. Moritomi, I. Kawano, S. Hamaguchi, A. Ishimatsu, T. Muramatsu, Catalase- and superoxide dismutase-induced morphological changes and growth inhibition in the red tide phytoplankton *Chattonella marina*, Biosci. Biotechnol. Biochem. 59 (1995) 2044–2048.
[31] R. Hema, M. Senthil-Kumar, S. Shivakumar, P. Chandrasekhara Reddy, M. Udayakumar, R.H.M.S.S. Shivakumar, P.C.R.M. Udayakumar, *Chlamydomonas reinhardtii*, a model system for functional validation of abiotic stress responsive genes, Culture 226 (2007) 655–670.
[32] F.C. Kupper, E. Gaquerel, A. Cosse, F. Adas, A.F. Peters, D.G. Muller, B. Kloareg, J.-P. Salaun, P. Potin, Free fatty acids and methyl jasmonate trigger defense reactions in *Laminaria digitata*, Plant Cell Physiol. 2009 (50) (2009) 789–800.
[33] I. Kawano, T. Oda, A. Ishimatsu, T. Muramatsu, Inhibitory effects of the iron chelator Desferrioxamine (Desferal) on the generation of activated oxygen species of *Chattonella marina*, Mar. Biol. 126 (1996) 765–771.
[34] T. Oda, A. Nakamura, M. Shikayama, I. Kawano, A. Ishimatsu, T. Muramatsu, Generation of reactive oxygen species by raphidophycean phytoplankton, Biosci. Biotechnol. Biochem. 61 (1997) 1658–1662.
[35] A.E. Allen, J. Laroche, U. Maheswari, M. Lommer, N. Schauer, P.J. Lopez, G. Finazzi, A.R. Fernie, C. Bowler, Whole-cell response of the pennate diatom *Phaeodactylum tricornutum* to iron starvation, Proc. Natl. Acad. Sci. U. S. A. 105 (2008) 10438–10443.
[36] L.V. Bindschedler, J. Dewdney, K.A. Blee, J.M. Stone, T. Asai, J. Plotnikov, C. Denoux, T. Hayes, C. Gerrish, D.R. Davies, F.M. Ausubel, G.P. Bolwell, Peroxidase-dependent apoplastic oxidative burst in Arabidopsis required for pathogen resistance, Plant J. 2006 (47) (2006) 851–863.
[37] R.R.L. Guillard, J.H. Ryther, Studies of marine planktonic diatoms: I. *Cyclotella nana* Hustedt, and *Detonula confervacea* (Cleve) Gran, Can. J. Microbiol. 8 (1962) 229–239.
[38] W. P. Inskeep and P. R. Bloom (1985) Extinction coefficients of chlorophyll a and b in N,N-dimethylformamide and 80% acetone. Plant Physiol., 1985, 77, 483–5.
[39] C. Ramakers, J.M. Ruijter, R.H.L. Deprez, A.F.M. Moorman, Assumption-free analysis of quantitative real-time polymerase chain reaction (PCR) data, Neurosci. Lett. 339 (2003) 62–66.
[40] M.W. Pfaffl, A new mathematical model for relative quantification in real-time RT-PCR, Nucleic Acids Res. 29 (2001) 2001–2007.
[41] A. Gruber, P. Kroth, M. Sachse, S. Sturm, Identification and evaluation of endogenous reference genes for steady state transcript quantification by qRT-PCR in the diatom *Phaeodactylum tricornutum* with constitutive expression independent from time and light, Endocytobiosis cell Res. J. Int. Soc. Endocytobiol. 24 (2013) 1–7.